18TH WORLD CONFERENCE ON EARTHQUAKE ENGINEERING
WCEE2024
MILAN

MILAN, ITALY
30TH JUNE - 5TH JULY 2024
www.wcee2024.it

EVALUATION OF THE CHORD ROTATION ACCORDING TO 2ND GENERATION OF EUROCODE 8 USING NONLINEAR ANALYSIS

H. Maranhão[1], H. Varum[2] & J. Melo[3]

[1] CONTRUCT-LESE, Faculty of Engineering of the University of Porto, Porto, Portugal, helder.maranhao@fe.up.pt

[2] CONTRUCT-LESE, Faculty of Engineering of the University of Porto, Porto, Portugal

[3] CONTRUCT-LESE, Faculty of Engineering of the University of Porto, Porto, Portugal

Abstract: *In recent decades, seismic engineering has evolved based on theoretical and experimental research and feedback from designers. Technological advancements in materials, structural solutions, and design methodologies have propelled the evolution of seismic codes, such as Eurocode 8, which is currently under revision. This revision aims to validate design parameters for reinforced concrete building sections. This article analyses and compares the beams' and columns' chord rotation for two reinforced concrete frame structures. This comparison is made by accessing the chord rotation of the respective elements through nonlinear analysis for ductility classes DC2 and DC3 and comparing them with the ones calculated as preconised in the second generation of Eurocode 8 part 1-1. The study reveals a moderate correlation between the calculated chord rotations using Eurocode 8 and those obtained through nonlinear analysis for the beams but a higher dispersion for the columns.*

1. General considerations

Recent advancements in research and development methodologies have impacted structural engineering design. This progress encompasses theoretical, experimental, and numerical investigations. Collaboration between researchers and practitioners has been critical to these efforts, introducing new construction materials, innovative structural solutions, and the evolution of design approaches within the engineering community. Simultaneously, evaluating the effects of recent seismic events on existing structures is paramount, offering valuable insights into their behaviour and identifying potential hazards. This comprehension subsequently guides the formulating of strategies and methodologies for reinforcing existing structures and devising plans for new ones. This continual evolution has necessitated the revision of design codes, particularly emphasising Eurocode 8. The ongoing progression has led to the need to update design codes, notably focusing on Eurocode 8, leading to the need to develop its second generation. Valuing the values and constraints associated with diverse parameters is crucial, particularly in the sections dedicated to reinforced concrete (RC) building design.

The objective of this study is to compare the chord rotation at yield (θ_y) and plastic chord rotation capacity (θ_u^{pl}) preconised in FprEN 1998-1-1(2024) with the chord rotation at yield ($\theta_{y,NL}$) and plastic chord rotation capacity ($\theta_{u,NL}^{pl}$) assessed by nonlinear analysis.

According to prEN 1998-1-2(2023), ensuring sufficient ductility and plastic rotation capacity in all critical regions of the beams is necessary. To achieve this, the product of the global displacement ductility factor, calculated as the product of the components of the behaviour factor q_R and q_D, and the chord rotation at yield (θ_y) of each member end should not exceed the chord rotation for the Significant Damage (SD) Limit State (θ_{SD}).

For the verification of SD, the resistance of ductile mechanisms should be taken as given by expression (1), as defined in FprEN 1998-1-1(2024):

$$\theta_{SD} = \frac{1}{\gamma_{Rd}} \cdot \left(\theta_y + \alpha_{SD,\theta} \cdot \theta_u^{pl}\right) \quad (1)$$

The parameter $\alpha_{SD,\theta}$ is the portion of the plastic chord rotation capacity $\theta_u^{pl} = \theta_u - \theta_y$ that corresponds to the attainment of SD, and γ_{Rd} is a partial factor on resistance at the SD limit state.

To provide a visual representation of the chord rotation in structures, Figure 1 depicts a schematic representation of the chord rotation at the left (θ_a) and right (θ_b) ends of beams and at the bottom (θ_c) and top (θ_d) ends of columns.

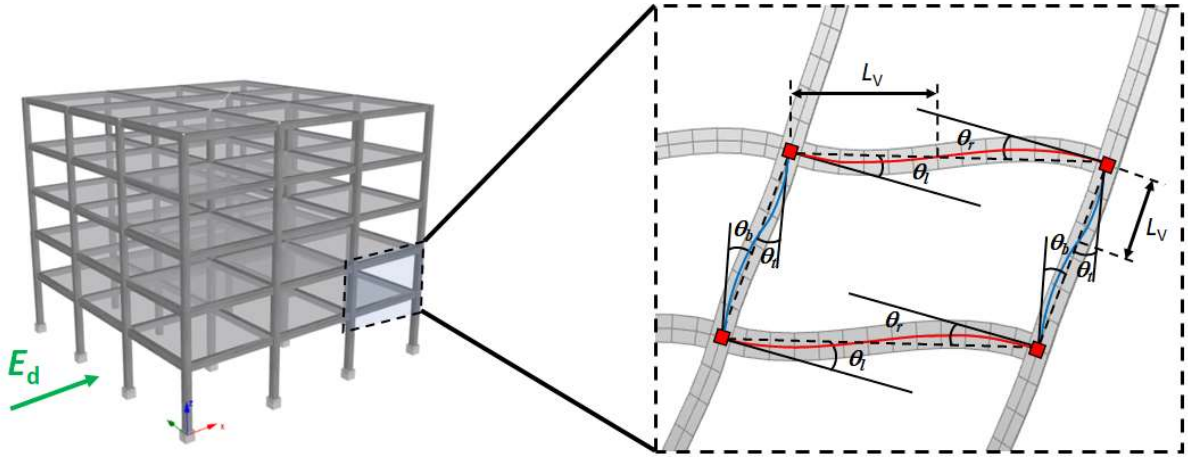

Figure 1. Schematic representation of the chord rotation [adapted from Maranhão et al.*(2023)]*

The chord rotation of the shear span (L_V=M/V) at yield (θ_y) for rectangular beams and columns may be evaluated according to expression (2), as proposed in FprEN 1998-1-1(2024):

$$\theta_y = \phi_y \cdot \frac{L_V + a_l}{3} + \frac{\phi_y \cdot d_{bL} \cdot f_y}{8 \cdot \sqrt{f_c}} + 0{,}0019 \cdot \left(1 + \frac{h}{1{,}6 \cdot L_V}\right) \quad (2)$$

The parameter ϕ_y is the yield curvature of the member in the end section. The tension shift of the bending moment diagram (a_l) is defined in the second generation of Eurocode 2 as being the same expression as in the current EN 1992-1-1(2004). The shear span (L_V) adopted for columns is half the clear height, as Fardis et al.(2015) referred to. The parameters f_y and f_c are the mean yield and compressive strength values of reinforcement steel and concrete, respectively. According to FprEN 1998-1-1(2024), plastic chord rotation capacity is defined according to equation (3):

$$\theta_u^{pl} = \kappa_{conform} \cdot \kappa_{axial} \cdot \kappa_{reinf} \cdot \kappa_{concrete} \cdot \kappa_{shearspan} \cdot \kappa_{confinement} \cdot \theta_{u0}^{pl} \quad (3)$$

where θ_{u0}^{pl} is the basic value of a member's plastic chord rotation capacity, taking the value of 0,039 rad if the member is a beam or a column with a section consisting of rectangular parts. The $\kappa_{conform}$ is the correction factor conforming whether is to DC1, DC2 or DC3; κ_{axial} is the correction factor for an axial force different than zero; κ_{reinf} is the correction factor for asymmetrical reinforcement; $\kappa_{concrete}$ is the correction factor for concrete strength other than 25 MPa; $\kappa_{shearspan}$ is the correction factor for a shear span-to-depth and $\kappa_{confinement}$ is the correction factor taking into account the confinement of concrete due to transverse bars.

2. Object of analysis

The structures included in this study consist of two five-storey buildings designed for DC2 and DC3 ductility classes, as illustrated in Figure 2. These structures were designed strictly to the standards outlined in FprEN 1998-1-1(2024), prEN 1998-1-2(2023), and EN 1992-1-1(2004). Additionally, the design response spectra were obtained following the EN 1998-1(2004) to establish a comprehensive beam and column analysis database.

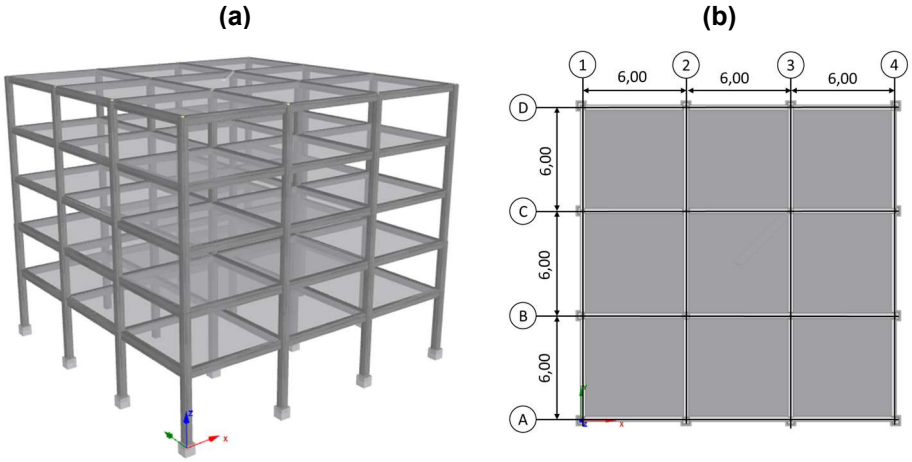

Figure 2. Five-storey building (a) Planview(b)

The structural system for the buildings consists of a series of frames with an equal spacing of 6,0 m, typical of residential buildings. The floor-to-floor height is 3,0 m for all storeys, except for the ground storey, which is 4,0 m. The solid slab thickness is 15,0 cm at each storey. The building's seismic response parameters are summarised in Table 1.

Table 1. Structure's seismic response parameters

Structures Label	Ductility Class	Number of Storeys	Total Height (m)	T_1 (s)	$S_d(T_1)$ (m/s^2)	V_b (kN)	d_{eroof} (m)
DC2-S5-0,5g	DC2	5	16	1,43	0,69	866,51	0,051
DC3-S5-0,5g	DC3			1,49	0,43	532,37	0,033

For all primary seismic members (beams, columns, and walls) for the buildings under analysis, it is considered the following materials:

- Concrete C30/37
- Reinforcement steel B500

The mechanical properties of concrete are defined according to EN 1992-1-1(2004) and EN 206-1(2007) standards. The steel reinforcement used for the present work is denominated as B500, and its mechanical properties are characterised according to EN 10080(2005). The database included 160 RC column specimens, biaxially loaded with squared cross-sections and 240 beams with rectangular cross-sections.

3. Methodology of analysis

The chord rotation at yielding (θ_y) and the plastic chord rotation capacity (θ_u^{pl}) are determined according to the specifications in FprEN 1998-1-1(2024). As referred to in section 1, this study aims to compare the chord rotation at yielding (θ_y) and the plastic chord rotation capacity (θ_u^{pl}) recommended in FprEN 1998-1-1(2024) with the chord rotation at yielding ($\theta_{y,NL}$) and the plastic capacity of the chord rotation ($\theta_{u,NL}^{pl}$), obtained through nonlinear analysis. The chord rotation at yield ($\theta_{y,NL}$) and the plastic chord rotation capacity ($\theta_{u,NL}^{pl}$) were estimated through nonlinear finite element modelling.

3.1. Adopted nonlinear analysis – Adaptive pushover

The adopted nonlinear analysis procedure in the present analysis is known as adaptive pushover analysis recurring to finite element software SeismoStruct from Seismosoft(2022). According to Seismosoft(2022), loads are applied to the structure in this type of analysis, like in conventional pushover analysis. However, in adaptive pushover analysis, it is crucial to model the inertia mass of the structures accurately to enable eigenvalue analysis, which is utilised in updating the loading vector.

In the case of force-based adaptive pushover analysis, it's essential to appropriately distribute mass across the nodes where incremental loads are to be applied. This ensures that the incremental forces can be accurately determined.

The adaptive load control and adaptive response control loading/solution procedures are employed instead of the load control and response control phases. Their input and functionality remain the same. However, it is noteworthy that in adaptive pushover analysis, only one adaptive phase (either load or response control) can be applied, unlike conventional pushover analysis, where multiple load or response control phases can be used simultaneously, as Seismosoft(2022) referred to.

3.2. Nonlinear finite element models definition

The nonlinear models were developed using SeismoStruct, developed by Seismosoft(2022), as shown in Figure 2. The analysis combines the 5 integration sections with 150 fibres in each integration section through the distributed fibre formulation approach.

The integration sections are located along the columns and beams in the distributed fibre formulation, as depicted in Figure 3.

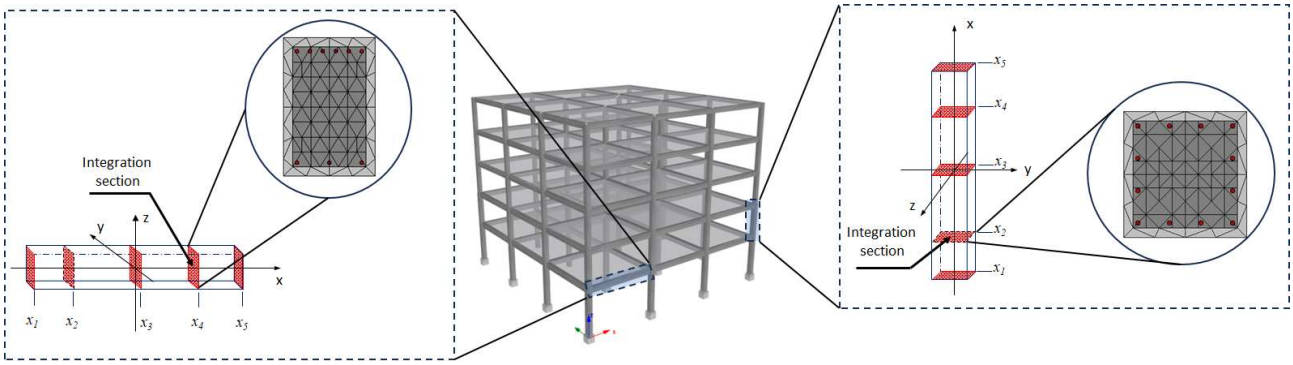

Figure 3. Schematic illustration of 5 integration sections and meshing for 150 fibres

The distributed inelasticity in elements using the force-based approach was implemented according to Neuenhofer and Filippou's(1997) formulation. In a force-based element, equilibrium is strictly satisfied, and no restraints are placed on developing inelastic deformations throughout the member.

3.3. Material constitutive models

The following subsections consider and describe constitutive models used for nonlinear analysis.

3.3.1. Concrete

The concrete constitutive relationship proposed by Mander et al.(1988) is a uniaxial nonlinear constant confinement model (Figure 4(a)). The confinement effects provided by the lateral transverse reinforcement are incorporated, whereby constant confining pressure is assumed throughout the stress-strain range. The concrete compressive strength considered in the analysis is the mean characteristic cylinder compressive strength. In the case of a concrete C30/37, the value of f_{cm}=38 MPa and its constitutive law is depicted in Figure 4(b).

A stress-strain model is developed for concrete subjected to uniaxial compressive loading and confined by transverse reinforcement. According to Mander et al.(1988), the model allows for cyclic loading and includes the strain rate effect. The influence of various types of confinement is considered by defining an effective lateral confining stress, which depends on the configuration of the transverse and longitudinal reinforcement.

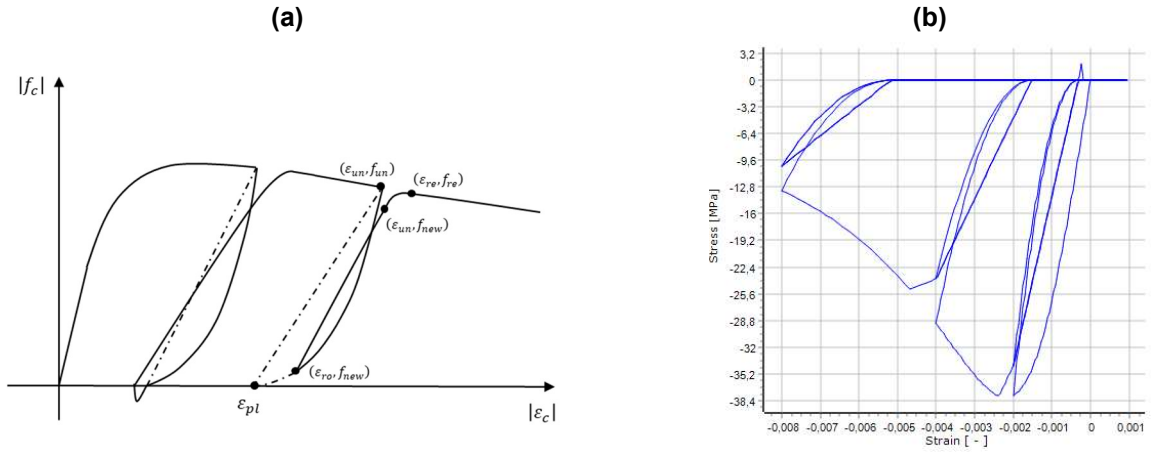

Figure 4. Concrete stress-strain curve (a) Proposed by Manderet al.(1988); (b) Actual curve used for finite element modelling

3.3.2. Reinforcement steel

The constitutive relationship for steel was initially programmed by Menegotto and Pinto(1973) and coupled with the isotropic hardening rules proposed by Taucer et al.(1991), as represented in Figure 5(a). The uniaxial steel model can reproduce the behaviour of different types of steel with good approximation. The constant *b* defines the slope of the hardening line. The exponent *R*, which varies after every inversion, affects the curvature of the diagram to represent the Bauschinger effect, according to Menegotto and Pinto(1973). Figure 5(b) shows the actual steel stress-strain curve used for nonlinear finite element modelling. The yield strength of the reinforcement considered in the analysis is the mean yield strength, as Maranhão et al.(2021) referred to. For B500 grade reinforcement steel, the mean value is f_{ym}≈555 MPa.

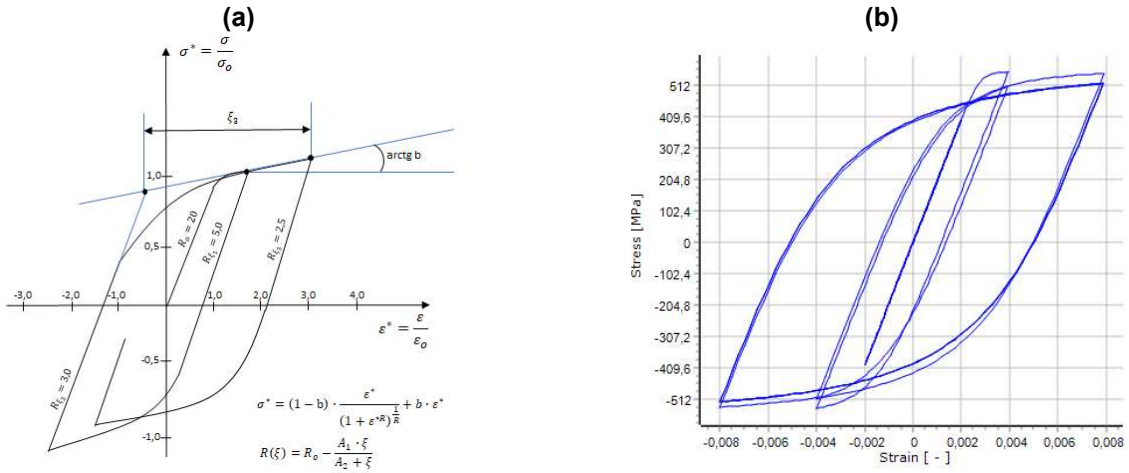

Figure 5. Steel stress-strain curve (a) Proposed by Menegotto and Pinto(1973) (b) Actual curve used in finite element modelling

3.4. Chord rotation calculation criteria by nonlinear assessment

The performance of the beams and columns was assessed following bilinearisation. This assessment followed the methodology outlined in FprEN 1998-1-1(2024). The yield chord rotation ($\theta_{y,NL}$) was determined to correspond to the attainment of an effective yield strength, M^*_y; it is linked to the elastic stiffness, K_e, as outlined in FprEN 1998-1-1 (2024).

The ultimate chord rotation ($\theta_{u,NL}$) is determined as the point at which the rotational strength (M) decreases by 20% relative to the maximum rotational strength (M_{max}), as shown in Figure 6(a). In cases where no decrease in lateral strength is observed, the ultimate chord rotation ($\theta_{u,NL}$) is considered to be at the maximum rotational strength (M_{max}), as illustrated in Figure 6(b).

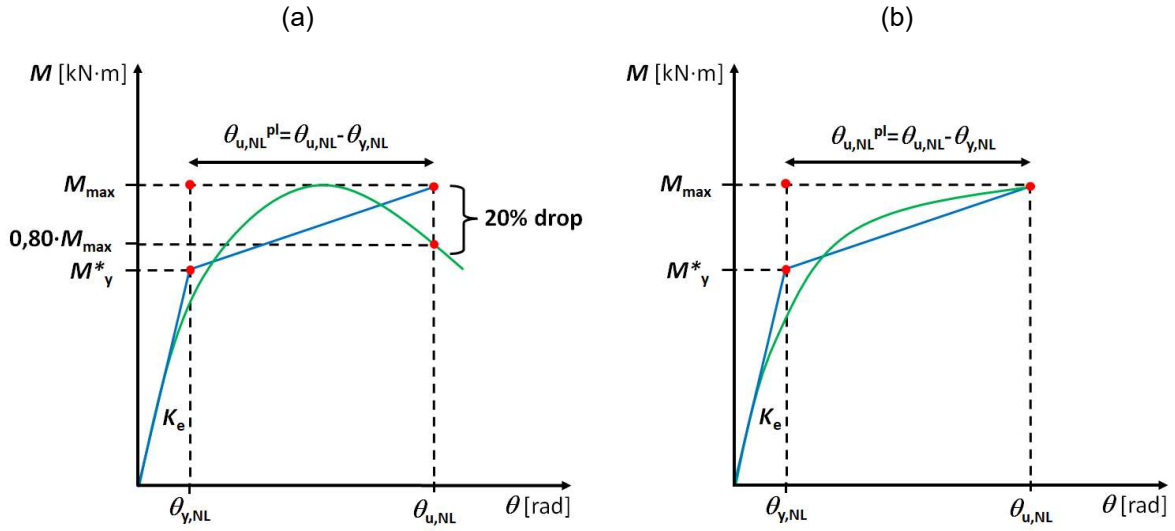

Figure 6. Bilinear idealisation of elements responses (a) with and (b) without drop in rotational strength after reaching the peak rotational strength

The plastic chord rotation capacity ($\theta_{u,NL}^{pl}$) is calculated as being the difference between the ultimate chord rotation ($\theta_{u,NL}$) and the chord rotation at yield ($\theta_{y,NL}$) at the end of the member, as defined by expression (4):

$$\theta_{u,NL}^{pl} = \theta_{u,NL} - \theta_{y,NL} \tag{4}$$

4. Results and conclusions

The following plots show the comparison between the chord rotation at yielding (θ_y) and plastic chord rotation capacity (θ_u^{pl}) preconised in FprEN 1998-1-1(2024) with the chord rotation at yielding ($\theta_{y,NL}$) and plastic chord rotation capacity ($\theta_{u,NL}^{pl}$) assessed by nonlinear analysis for the beams.

It is important to note that the dataset in this article is relatively limited. To enhance result accuracy, one should consider expanding the dataset. The author is working on a significantly broader dataset encompassing various types of buildings.

Regarding the analysis of the chord rotation, as illustrated in Figure 7 and Figure 8, it can be observed differences in the dispersion of points for chord rotation components, calculated from equations (2) and (3), preconised in FprEN 1998-1-1(2024), and those obtained through pushover analysis can be attributed to various factors such as

a) Equations (2) and (3) are simplified analytical expressions, while pushover analysis accounts for more realistic factors, resulting in divergent outcomes.

b) Nonlinear analysis requires intricate modelling, considering material nonlinearity, geometric nonlinearities, and boundary conditions. Analytical equations may disregard these complexities, leading to disparities.

c) Pushover analysis employs numerical methods to solve nonlinear equations, capturing additional intricacies that analytical equations may not encompass.

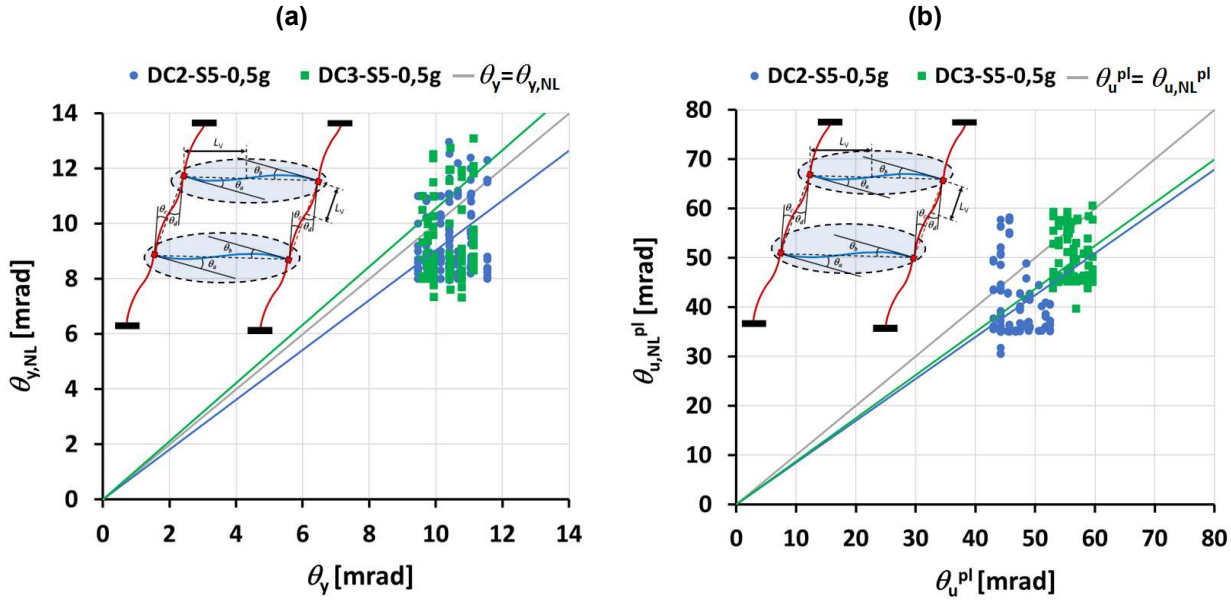

Figure 7. Beams chord rotation (a) θ_y vs $\theta_{y,NL}$ (b) θ_u^{pl} vs $\theta_{u,NL}^{pl}$

Regarding the pairs of values (θ_y;$\theta_{y,NL}$) from Figure 7(a) and (θ_u^{pl};$\theta_{u,NL}^{pl}$) from Figure 7 (b), a paired *t*-test was employed. The *t*-test in the context of correlation is used to determine whether the correlation coefficient calculated from the sample is significantly different from zero, suggesting whether there is a significant linear relationship between the pairs of variables under analysis. Regarding the beam's chord rotations dataset, as illustrated in Figure 7, we can draw the following conclusions:

a) The data set from Figure 7(a), for DC2-S5-0,5g and DC3-S5-0,5g, the *p*-value less than 0,01, suggests that the correlation coefficient is statistically significant at the 1,0% significance level. In that case, one would reject the null hypothesis and conclude that there is a considerable correlation between θ_y and $\theta_{y,NL}$.

b) Comparing how the data points are distributed relative to the 45-degree line ($\theta_y = \theta_{y,NL}$) in Figure 7(a), the trend lines show that DC2-S5-0,5g differs by about 13%, and DC3-S5-0,5g differs by approximately

7%. The datasets have their points clustered moderately around the 45-degree line; it suggests a moderate linear relationship close to the ideal.

c) As per Figure 7(b), the *p*-value for the pairs (θ_u^{pl} and $\theta_{u,NL}^{pl.}$) is less than 0,01, suggesting that the correlation coefficient is statistically significant at the 1,0% significance level.

d) Regarding the 45-degree line ($\theta_u^{pl} = \theta_{u,NL}^{pl}$), the trend lines for DC2-S5-0.5g exhibit a difference of approximately 18%, while DC3-S5-0,5g shows a variance of nearly 16% from the slope of the 45-degree line. The datasets demonstrate a moderate clustering of points around the 45-degree line, indicating a moderate linear relationship close to the ideal.

e) Considering these comparisons, we can conclude that DC3-S5-0,5g has a higher linear relationship for the pairs (θ_u^{pl};$\theta_{u,NL}^{pl}$) than DC2-S5-0,5g. Therefore, based on the provided data, it's reasonable to affirm that DC3-S5-0,5g is more ductile than DC2-S5-0,5g regarding the beam's chord rotation.

The following plots show the comparison between the chord rotation at yielding (θ_y) and plastic chord rotation capacity (θ_u^{pl}) preconised in FprEN 1998-1-1(2024) with the chord rotation at yielding ($\theta_{y,NL}$) and plastic chord rotation capacity ($\theta_{u,NL}^{pl,}$) assessed by nonlinear analysis for the beams.

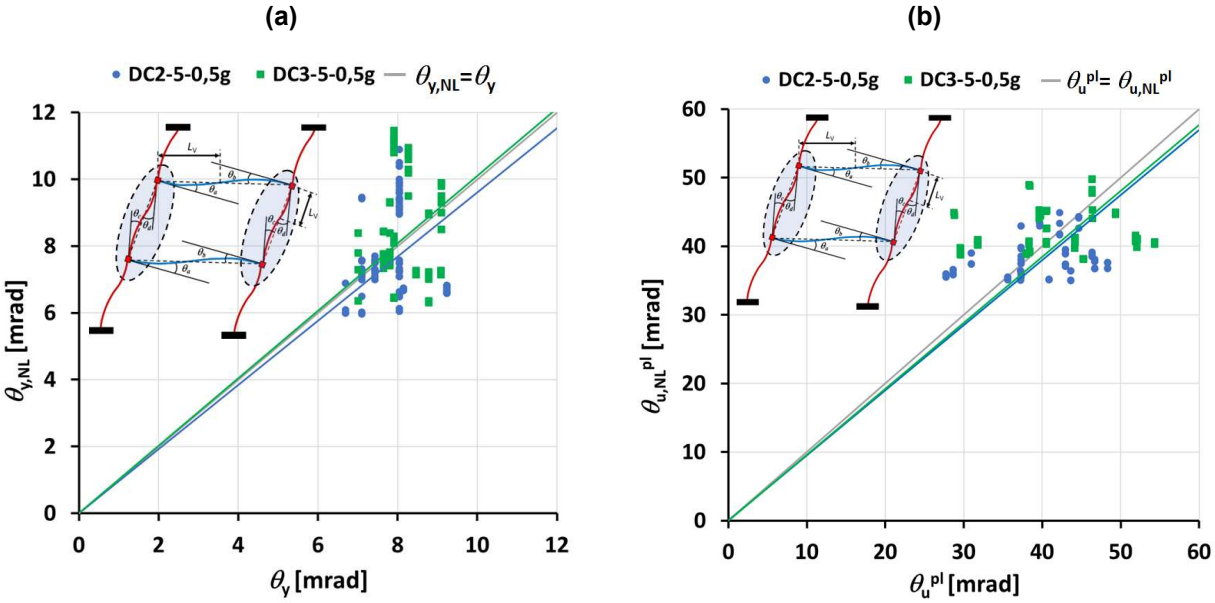

Figure 8. Columns chord rotation (a) θ_y vs $\theta_{y,NL}$ (b) θ_u^{pl} vs $\theta_{u,NL}^{pl}$

Regarding the pairs of values (θ_y;$\theta_{y,NL}$) from Figure 8 (a) and (θ_u^{pl};$\theta_{u,NL}^{pl}$) from Figure 8 (b), a paired *t*-test was also employed. Regarding the data from Figure 8, the following observations can be made:

a) The dataset extracted from Figure 8(a) reveals that for DC2-S5-0,5g and DC3-S5-0,5g, the calculated *p*-value being less than 0,01 indicates a statistically significant correlation coefficient at the 1,0% significance level. This observation concludes that a significant correlation exists between θ_y and $\theta_{y,NL}$.

b) The trend lines of Figure 8(a) show that DC2-S5-0,5g differ by about 6% and DC3-S5-0,5g differ by approximately 2% from the slope of the 45-degree line (θ_y=$\theta_{y,NL}$). The datasets have their points clustered closely around the 45-degree line; it suggests a moderate linear relationship close to the ideal.

c) Regarding Figure 8(b), the trend line for DC2-S5-0.5g differs by about 4%, and DC3-S5-0,5g varies about 2% from the slope of the 45-degree line (θ_u^{pl} =$\theta_{u,NL}^{pl}$). The datasets have their points clustered moderately around the 45-degree line; it suggests a moderate linear relationship close to the ideal.

d) Based on these comparisons, it can be inferred that DC3-S5-0,5g exhibits a stronger linear relationship for the pairs (θ_u^{pl}=$\theta_{u,NL}^{pl}$) than DC2-S5-0,5g. Consequently, considering the provided data, it is

reasonable to assert that DC3-S5-0,5g demonstrates higher ductility than DC2-S5-0,5g concerning the column's chord rotation.

In summary, the analysis compares the chord rotation at yield (θ_y) and plastic chord rotation capacity (θ_u^{pl}) calculated according to FprEN 1998-1-1(2024) and the ones obtained by nonlinear analysis for DC2-S5-0,5g and DC3-S5-0,5g. Both datasets exhibit a moderate positive linear relationship between these parameters. DC3-S5-0,5g shows a slightly stronger correlation and less dispersion than DC2-S5-0,5g.

Based on the analysis, DC3-S5-0,5g demonstrates higher plastic chord rotation capacity than DC2-S5-0,5g. This conclusion suggests that DC3-S5-0,5g possesses higher ductility in line with the provisions of FprEN 1998-1-1 (2024) and prEN 1998-1-2(2023).

5. Acknowledgements

This work is financially supported by national funds through the FCT/MCTES (PIDDAC) under the project 2022.05721.PTDC – AR-SeismicRC – Assessment and retrofitting of non-seismically conforming existing reinforced concrete building structures and validation of the corresponding Eurocode 8-3 recommendations, and by Base Funding - UIDB/04708/2020 and Programmatic Funding - UIDP/04708/2020 of the CONSTRUCT - Instituto de I&D em Estruturas e Construções - funded by national funds through the FCT/MCTES (PIDDAC).

6. References

EN 206-1 (2007) *Concrete - Part 1: Specification, performance, production and conformity*. Brussels: CEN-European Committee for Standardization.

EN 1992-1-1 (2004) *Eurocode 2: Design of concrete structures - Part 1-1 : General rules and rules for buildings*. Brussels: CEN-European Committee for Standardization.

EN 1998-1 (2004). Brussels: CEN-European Committee for Standardization.

EN 10080 (2005) *Steel for the reinforcement of concrete - Weldable reinforcing steel - General*, *ISE/104*. Brussels: CEN-European Committee for Standardization.

FprEN 1998-1-1 (2024) *Eurocode 8: — Design of structures for earthquake resistance — Part 1-1: General rules and seismic action*. Brussels: CEN/TC 250/SC 8.

Mander, J.B., Priestley, M.J.N. and Park, R. (1988) 'Theoretical Stress-Strain Model for Confined Concrete', *ASCE Journal of Structural Engineering*]. Available at: https://doi.org/10.1061/(asce)0733-9445(1988)114:8(1804).

Maranhão, H. *et al.* (2023) 'Comparative analysis of the impact of design and detailing provisions for RC moment resisting frames under the first- and second-generation of Eurocode 8', *Engineering Structures*. Available at: https://doi.org/(Not yet published).

Menegotto, M. and Pinto, P.E. (1973) 'Method of Analysis for Cyclically Loaded R. C. Plane Frames Including Changes in Geometry and Non-Elastic Behavior of Elements under Combined Normal Force and Bending', in *Proceedings of IABSE Symposium on Resistance and Ultimate Deformability of Structures Acted on by Well Defined Loads*, pp. 15–22. Available at: https://doi.org/10.5169/seals-13741.

Neuenhofer, A. and Filippou, F.C. (1997) 'Evaluation of Nonlinear Frame Finite-Element Models', *Journal of Structural Engineering* [Preprint]. Available at: https://doi.org/10.1061/(asce)0733-9445(1997)123:7(958).

prEN 1998-1-2 (2023) *Eurocode 8: Design of structures for earthquake resistance - Part 1-2: Rules for new buildings*. Brussels: CEN/TC250/SC8.

Seismosoft (2022) 'SeismoStruct 2022 – A computer program for static and dynamic nonlinear analysis of framed structures'. Seismosoft. Available at: https://seismosoft.com/.